



Contents lists available at ScienceDirect

## Bioorganic &amp; Medicinal Chemistry Letters

journal homepage: [www.elsevier.com/locate/bmcl](http://www.elsevier.com/locate/bmcl)

## From virtual to clinical: The discovery of PGN-1531, a novel antagonist of the prostanoid EP<sub>4</sub> receptor



Jon Sutton<sup>a,\*</sup>, David E. Clark<sup>a</sup>, Christopher Higgs<sup>a,†</sup>, Marcel J. de Groot<sup>a</sup>, Neil V. Harris<sup>a</sup>, Andrea Taylor<sup>a</sup>, Peter M. Lockey<sup>a</sup>, Karen Maubach<sup>c</sup>, Amanda Woodroffe<sup>b,‡</sup>, Richard J. Davis<sup>b,§</sup>, Robert A. Coleman<sup>b,¶</sup>, Kenneth L. Clark<sup>b,||</sup>

<sup>a</sup>Argenta, 8/9 Spire Green Centre, Flex Meadow, Harlow, Essex CM19 5TR, United Kingdom

<sup>b</sup>Pharmagene plc, 2 Orchard Road, Royston, Hertfordshire SG8 5HD, United Kingdom

<sup>c</sup>BTG International Ltd, 5 Fleet Place, London EC4M 7RD, United Kingdom

## ARTICLE INFO

## Article history:

Received 8 January 2014

Revised 21 February 2014

Accepted 24 February 2014

Available online 12 March 2014

## Keywords:

EP<sub>4</sub> receptor antagonist

Hit-finding

Lead optimization

Migraine

Cerebral vasodilatation

## ABSTRACT

In this Letter, we present the results of a hit-finding and lead optimization programme against the EP<sub>4</sub> receptor (EP<sub>4</sub>R). In a short time period, we were able to discover five structurally diverse series of hit compounds using a combination of virtual screening methods. The most favoured hit, compound **6**, was demonstrated to be a competitive antagonist of the EP<sub>4</sub>R. Compound **73** was identified following several rounds of optimization, which centred on improving both the primary EP<sub>4</sub>R affinity and selectivity against the related EP<sub>2</sub>R as well as the aqueous solubility. This work culminated in the preparation of **PGN-1531**, the sodium salt of **73**, which showed a marked improvement in solubility (>10 mg/mL). **PGN-1531** is a potent and selective antagonist at EP<sub>4</sub>Rs in vitro and in vivo, with the potential to alleviate the symptoms of migraine that result from cerebral vasodilatation.

© 2014 Elsevier Ltd. All rights reserved.

The prostanoid receptor subfamily comprises nine members: DP, EP<sub>1–4</sub>, FP, IP, TP and the more recently identified CRTH2.<sup>1</sup> The EP receptors (for which the endogenous ligand is PGE<sub>2</sub>) have been cloned and are distinct at both a molecular and pharmacological level.<sup>2</sup> EP<sub>4</sub> receptor (EP<sub>4</sub>R) antagonists have been shown to have potential in the treatment of inflammatory pain<sup>3</sup> and, in particular, in the treatment of primary headache disorders, which include migraines, and secondary headache disorders, such as drug-induced headaches.<sup>4</sup> Dilation of the cerebral vasculature and the subsequent activation of pain-stimulating, perivascular trigeminal sensory afferent nerves is recognised to play an important role in the pathophysiology of migraine. A sterile inflammatory response,

\* Corresponding author. Tel.: +44 (0) 1279 645645; fax: +44 (0) 1279 645 646.

E-mail address: [jon.sutton@crl.com](mailto:jon.sutton@crl.com) (J. Sutton).

† Current address: Schrödinger, Inc., 120 West 45th Street, 17th Floor, New York, NY 10036, USA.

‡ Current address: Stemgent/Asterand, 2A Orchard Road, Royston, Hertfordshire SG8 5HD, United Kingdom.

§ Current address: Investment Division, The Wellcome Trust, 215 Euston Road, London NW1 2BE, United Kingdom.

¶ Current address: 27 Wodehouse Terrace, Falmouth, Cornwall TR11 3EN, United Kingdom.

|| Current address: Department of Asthma and Allergy Biology, Respiratory and Inflammation CEDD, GlaxoSmithKline, Gunnels Wood Road, Stevenage, Hertfordshire SG1 2NY, United Kingdom.

associated with activation of cyclooxygenase and the generation of PGE<sub>2</sub>, is also implicated in the pathophysiology of migraine. PGE<sub>2</sub> levels have been shown to be raised during migraine attacks and PGE<sub>2</sub> contributes to the pain of migraine by directly dilating cerebral arteries and by stimulating the release of vasoactive/proinflammatory peptides from the trigeminal nerves. These effects of PGE<sub>2</sub> are mediated in whole or in part by EP<sub>4</sub>Rs. Thus, by binding to and preventing the stimulation of EP<sub>4</sub>Rs, EP<sub>4</sub>R antagonists may be used to treat the pain associated with migraine.

In this Letter, we describe the virtual screening and medicinal chemistry optimization that led to the discovery of **PGN-1531**, a novel, potent and selective EP<sub>4</sub>R antagonist.

The virtual screening campaign comprised two rounds of compound selection and acquisition over approximately seven months. Following a review of the relatively sparse literature available at the time concerning EP<sub>4</sub>R antagonists, four compounds were chosen as the basis for virtual screening (compounds **1–4**, Table 1).

Various virtual screening approaches were applied including 2-D and 3-D ligand-based searches together with docking into an EP<sub>4</sub>R homology model. Following assessment of compounds selected from these searches by an experienced medicinal chemist, a total of 516 compounds was ordered from commercial suppliers.

**Table 1**  
Chemical structures of the compounds used as queries in the first round of database searches

| Compound | Structure | Refs. |
|----------|-----------|-------|
| 1        |           | 5,6   |
| 2        |           | 7     |
| 3        |           | 8     |
| 4        |           | 9     |

Once the compounds from the first round of virtual screening had been screened, a second round of searches was carried out. The purpose of these searches was to exploit the emerging SAR information acquired from the screening of the first round of compounds and also to take advantage of new information in the literature concerning a previously undisclosed EP<sub>4</sub>R antagonist from Ono (Table 2). As a result of these searches, a further 363 compounds were ordered.

In all, the two rounds of compound selection led to a total of 879 compounds being ordered. In the final analysis, 762 of the 879 compounds (i.e., about 87%) were acquired from 12 suppliers.

Of the 762 compounds, six proved insufficiently soluble in DMSO to be screened, leaving 756 to be tested in the primary assay.<sup>11</sup> These compounds were screened at a single concentration of 10 μM. All compounds were also checked for purity and identity by LC/MS. For 36 compounds showing a sufficient level of inhibition at 10 μM (typically >ca. 40%), IC<sub>50</sub> values were determined using six-point concentration/inhibition curves. The breakdown of these results is shown in Table 3.

**Table 2**  
New antagonist structure

| Compound | Structure | Ref. |
|----------|-----------|------|
| 5        |           | 10   |

**Table 3**  
Summary of EP<sub>4</sub>R IC<sub>50</sub> values obtained in primary screening

| IC <sub>50</sub> range (μM) | Number of compounds in IC <sub>50</sub> range |
|-----------------------------|---|
| IC <sub>50</sub> > 25       | 5   |
| 10 < IC <sub>50</sub> ≤ 25  | 15  |
| 5 < IC <sub>50</sub> ≤ 10   | 8   |
| IC <sub>50</sub> ≤ 5        | 8   |

Based on the accumulated screening data, five series of compounds were identified as having potential for hit-to-lead exploration. Each series represented a tractable starting point for further optimisation, possessing low μM potency, favourable calculated physicochemical properties, generally good LE values and some early SAR data. The structure of the head compound of each series is shown in Table 4 together with associated biological data obtained from the screening sample.

From the viewpoint of novelty, the furan ether series, typified by compound 6, was particularly interesting and so the structure and activity of this compound were confirmed from a larger batch of material obtained from the supplier (giving an IC<sub>50</sub> value of 1.0 μM). These confirmatory results, together with some early SAR (Table 5), gave sufficient confidence in this series for it to form the basis of a hit-to-lead chemistry programme. Overall, the early SAR indicated the requirement for an acidic moiety (see 12) and a 1–4 biaryl ring system. Compound 6 was found to be selective over both EP<sub>1</sub>R and EP<sub>3</sub>R but not EP<sub>2</sub>R (95% inhibition at 10 μM), therefore the attainment of greater EP<sub>4</sub>R/EP<sub>2</sub>R selectivity was one of the goals of lead optimisation as well as boosting primary potency against the EP<sub>4</sub>R.

Encouragingly, a Scatchard kinetic analysis of compound 6 confirmed it as a competitive inhibitor of binding at the EP<sub>4</sub>R (Fig. 1). Additionally, the compound behaved as an antagonist in a functional cell-based assay<sup>12</sup> (pK<sub>b</sub> = 5.78 ± 0.39).

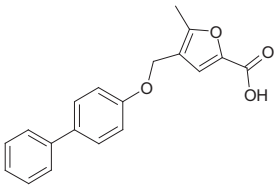
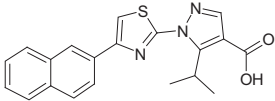
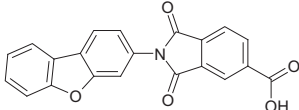
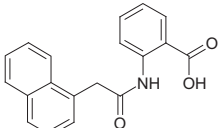
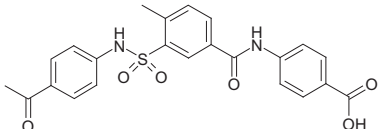
The data in Table 5 highlight the requirement for the carboxylic acid group, which can be rationalised by our EP<sub>4</sub>R homology model<sup>13,14</sup> (Fig. 2) in terms of the need for a strong interaction with Arg255 in the EP<sub>4</sub>R, and also a very specific arrangement of an approximately planar aromatic ring system at an appropriate distance from the carboxylate. A further hydrogen-bonding interaction between the ether linker in compound 6 and Tyr<sup>184</sup> can also be observed.

Early lead optimization of the furan ether hit 6 centred on variation of the furan core and the use of solid-phase library chemistry to the probe the SAR of the biaryl moiety, Figure 3.

The emerging early SAR shown in Table 6 indicated that simple variation of the 5-methyl substituent was tolerated (compounds 15–17). However, chain extension of the carboxylic acid from the furan core in compounds 18 and 19 led to some reduction in EP<sub>4</sub>R affinity, although replacing the acid with a tetrazole bioisostere led to a fivefold improvement in affinity (K<sub>i</sub> = 80 nM). Variation of the furan-ether linker showed a more marked SAR, with the amide 21 being inactive—although both the homologated ether and the amine-linked compounds 20 and 22, respectively, were found to have modest affinity compared to the virtual screening hit 6. After several rounds of modifications to the original hit compound, we identified a preference for the original hit scaffold, substituents and linking groups.

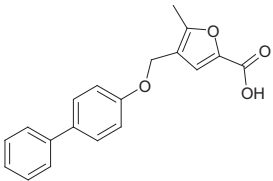
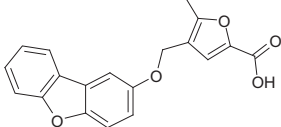
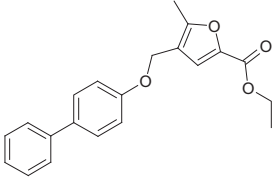
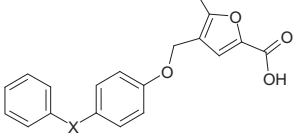
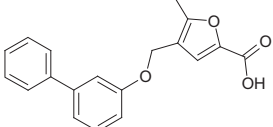
With this information in hand, we proceeded to examine variation of the biaryl system. The solid-supported chemistry utilized to expand the SAR around the biaryl moiety of compound 6 is shown in Scheme 1. The commercial furan alcohol 23 was TBDMS-protected and the core carboxylic acid installed using lithiation followed by addition of carbon dioxide to give compound 24. The attachment to 2-chlorotrityl chloride resin was then performed and the protecting group removed to give the alcohol 25.

**Table 4**  
Heads of the series identified as having potential for hit-to-lead exploration

| Series       | Compound | Head of Series  | EP <sub>4</sub> R IC <sub>50</sub> (μM) | <sup>a</sup> LE/LLE |
|--------------|----------|---|---|---------------------|
| Furan ethers | 6        |  | 2.4                                     | 0.35/1.66           |
| Pyrazoles    | 7        |  | 1.2                                     | 0.33/0.16           |
| Phthalimides | 8        |  | 0.46                                    | 0.32/2.36           |
| ortho-Amides | 9        |  | 2.6                                     | 0.33/0.94           |
| para-Amides  | 10       |  | 1.0                                     | 0.26/2.17           |

<sup>a</sup> LE = ligand efficiency index ( $1.4 \times (-\log IC_{50})$ )/number of heavy atoms); LLE = ligand lipophilicity index ( $EP_4R IC_{50} - c \text{ Log } P$ ).

**Table 5**  
Initial SAR for furan ether series

| Compound | Structure   | EP <sub>4</sub> R IC <sub>50</sub> (μM)                               |
|----------|---|---|
| 6        |  | 1   |
| 11       |  | 4.6   |
| 12       |  | 15% inh. @ 10 μM  |
| 13       |  | (X = O) 7% inh. @ 10 μM<br>(X = C(Me) <sub>2</sub> ) 23% inh. @ 10 μM |
| 14       |  | 10  |

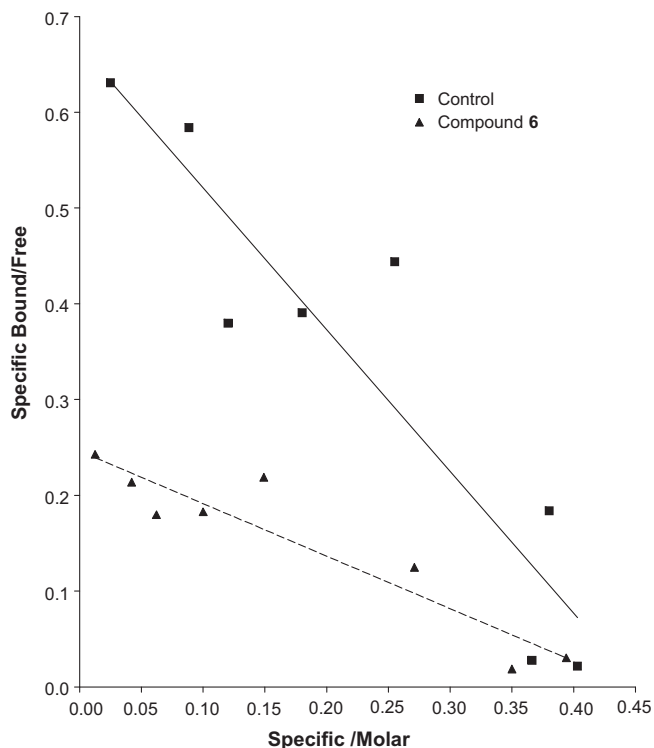


**Figure 1.** Scatchard analysis generated from [ $^3\text{H}$ ]-PGE $_2$  saturation binding data, in the absence and presence of 1  $\mu\text{M}$  of compound **6** ( $K_d = 1.7 \pm 0.2 \text{ nM}$ ,  $B_{\text{max}} = 0.4 \pm 0.03 \text{ nM}$ ).

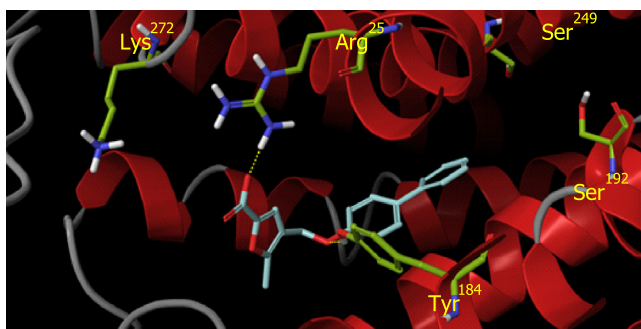


**Figure 2.** Binding mode of compound **6** (grey) showing binding to key residues in the EP $_4$ R homology model.

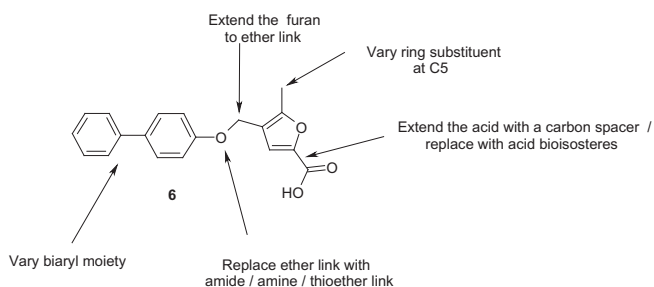


**Figure 3.** Areas of modification of original hit compound **6**.

A Mitsunobu coupling with 4-iodo-phenol gave the ether **26**, which was subsequently used to prepare an array of biaryl analogues using Suzuki–Miyaura coupling reactions of selected boronic acids.

**Table 6**  
Linker SAR and core template variation in furan ether series

| Compound  | R <sup>2</sup>  | X                                   | n | EP <sub>4</sub> R<br>K <sub>i</sub> ( $\mu\text{M}$ ) <sup>11</sup> |
|-----------|-----------------|-------------------------------------|---|---|
| <b>6</b>  | Me              |                                     | 0 | 0.42  |
| <b>15</b> | H               |                                     | 0 | 2   |
| <b>16</b> | <i>i</i> Pr     | –OCH <sub>2</sub> –                 | 0 | 3   |
| <b>17</b> | CF <sub>3</sub> |                                     | 0 | 1.3   |
| <b>18</b> | Me              |                                     | 1 | 61% inhib. @ 10 $\mu\text{M}$                                       |
| <b>19</b> | Me              |                                     | 2 | 63% inhib. @ 10 $\mu\text{M}$                                       |
| <b>20</b> | Me              | –OCH <sub>2</sub> CH <sub>2</sub> – | 0 | 3.8   |
| <b>21</b> | Me              | –CONH–                              | 0 | >30   |
| <b>22</b> | Me              | –NH–                                | 0 | 1.4   |

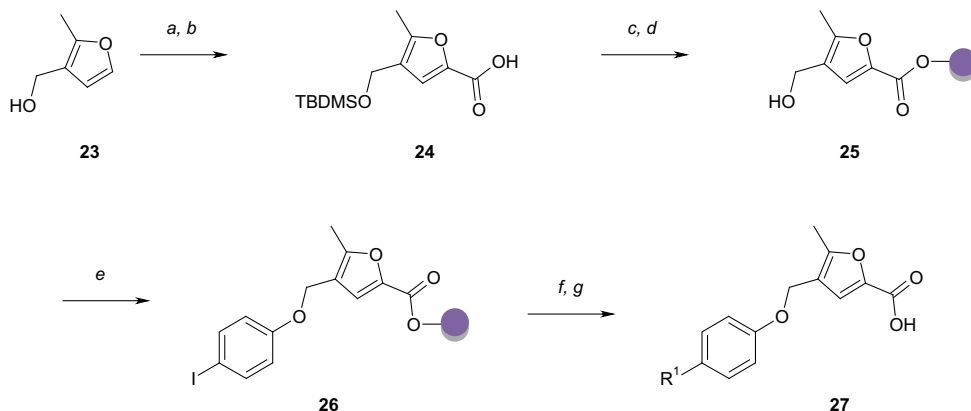
The array compounds **27** were obtained following cleavage from the resin using TFA/DCM.

Screening data from the biaryl compounds **28–48** (Table 7) showed that there was a clear preference for the more lipophilic and/or electron-donating substituents in biphenyl analogues such as the *para*-methoxy and *para*-di-fluoromethoxy compounds (entries **30** and **36**, respectively). It is possible that steric effects are responsible for the difference in activity of the 3,4-methylenedioxy compound **34** compared to the 3,4-dimethoxy analogue **33**, which shows a fivefold drop in EP $_4$ R affinity. A further examination of the data indicates that compounds in which the distal phenyl ring is substituted with polar groups are poorly tolerated (entries **40–42**) as well as compounds where the phenyl ring is replaced with various polar heterocycles (entries **43–47**). This presumably reflects the highly lipophilic nature of the binding site in this region of the EP $_4$ R. A notable exception to this observation is the *para*-methoxy pyridyl analogue **48**, which has improved affinity resulting from a favourable interaction of the *para*-methoxy substituent.

A SiteMap<sup>15</sup> binding site analysis is shown in Figure 4 for selected compounds **30**, **33**, **34** and **39**, which indicates that the binding region in the EP $_4$ R is highly hydrophobic, with the more potent analogues placing methyl groups in a hydrophobic area linked by an oxygen atom in an acceptor area, whereas the various less potent compounds place polar groups in hydrophobic areas. The high affinity exhibited by the phenyl methyl ketone **39** can be rationalized as the compound is able to pick up additional hydrophobic (methyl group) and hydrogen-bond acceptor (ketone oxygen) binding interactions.

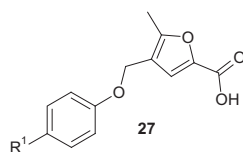
After the first rounds of early optimisation, the major goals were to increase EP $_4$ R affinity further and to improve EP $_4$ R/EP $_2$ R selectivity, which remained poor for most carboxylic acid-containing analogues (data not shown). To do this, we took advantage of a recently released structure (at the time) of a potent competitor compound from Ono<sup>10</sup> (**5**). The Ono compound was found to be very potent and selective in our hands, (EP $_4$ R  $K_i = 7 \text{ nM}$ ; >600-fold selectivity over the related EP $_2$ R). A simple FlexS<sup>16</sup> overlay of **5** (both R and S enantiomers are shown) with a proposed acylsulfonamide target **49**, derived from the original hit compound **6**, indicated that an acyl sulfonamide group may be able to pick up some additional interactions similar to those present in the highly EP $_4$ R selective Ono compound (Fig. 5).

Gratifyingly, the first acylsulfonamide compound **49** was found to have greatly improved affinity at EP $_4$ R and, very encouragingly, showed a marked improvement in EP $_4$ R/EP $_2$ R selectivity profile compared to the parent carboxylic acid **6** (Table 8). The LLE data indicate that compound **49** has a comparable value to the Ono compound **5**.



**Scheme 1.** Synthesis of phenoxy-methyl-furan-2-carboxylic acid array: (a) TBDMS-Cl, Imidazole, DMF, RT, 2 h (68%); (b) (i) *n*Bu-Li (2.5 M in hexanes), THF,  $-78^{\circ}\text{C}$ , 30 min, (ii)  $\text{CO}_2(\text{g})$  (30%); (c) 2-Chlorotrityl chloride resin (1.3 mmol/g), DCM; (d) TBAF, RT, 18 h; (e) 4-Iodo-phenol, triphenyl phosphine, DIAD, THF, RT, 16 h; (f)  $\text{R}^1\text{-B}(\text{OH})_2$ ,  $\text{PdCl}_2(\text{dppf})_2$ ,  $\text{Cs}_2\text{CO}_3$ , DMF,  $100^{\circ}\text{C}$ , 1 h (48–100%); (g) 5% TFA, DCM, RT, 20 min (65–85%).

**Table 7**  
Initial SAR from the furan ether array



| Compound | R <sup>1</sup> | EP <sub>4</sub> R<br>K <sub>i</sub> (μM) <sup>11</sup> | Compound | R <sup>1</sup> | EP <sub>4</sub> R<br>K <sub>i</sub> (μM) <sup>11</sup> |
|----------|----------------|--|----------|----------------|--|
| 6        |                | 0.42   | 38       |                | 1.5  |
| 28       |                | 10   | 39       |                | 0.15   |
| 29       |                | 3  | 40       |                | >>10   |
| 30       |                | 0.09   | 41       |                | >>10   |
| 31       |                | 0.74   | 42       |                | >>10   |
| 32       |                | 1.6  | 43       |                | >>10   |
| 33       |                | 2.8  | 44       |                | >>10   |
| 34       |                | 0.6  | 45       |                | >10  |
| 35       |                | 2.4  | 46       |                | >>10   |
| 36       |                | 0.02   | 47       |                | >>10   |
| 37       |                | 1  | 48       |                | 1.3  |

With these encouraging data in hand for compound **49**, we proceeded to incorporate elements identified from the early lead optimisation work into new acylsulfonamide analogues (Table 9, compound **50**). The results from acylsulfonamide compounds

prepared with variation to the distal phenyl ring culminated in some very potent and selective examples, with the di-fluoromethoxy acylsulfonamide **52** ( $K_i = 1.3$  nM) exhibiting a further 20-fold improvement in EP<sub>4</sub>R affinity compared to compound **49** (and

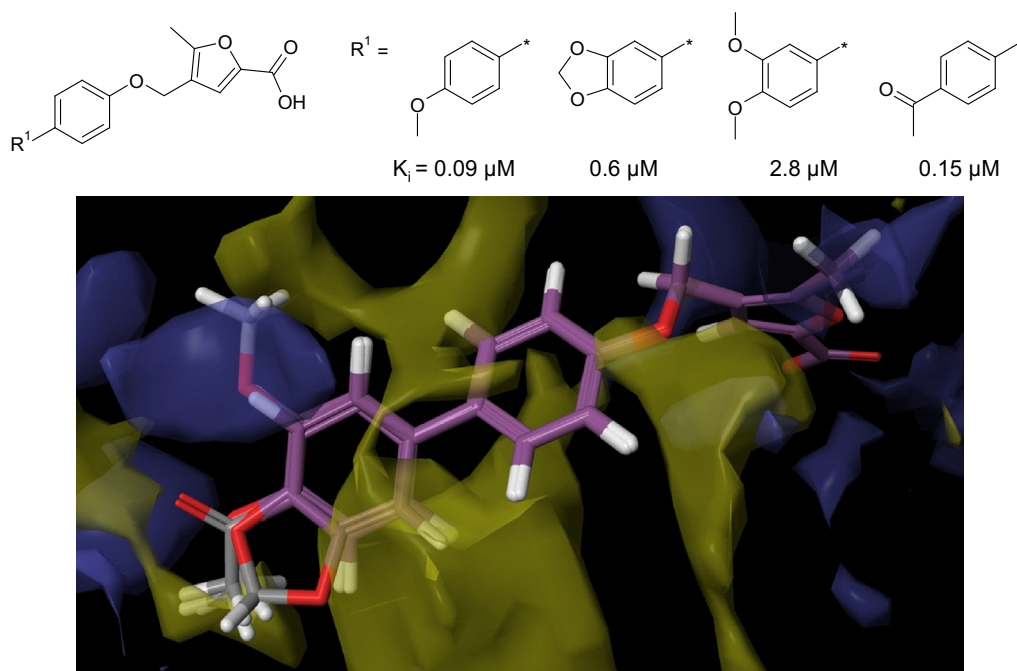


**Figure 4.** SiteMap binding site profile showing areas preferring hydrophobic (yellow) and hydrogen-bond acceptor (blue) groups.

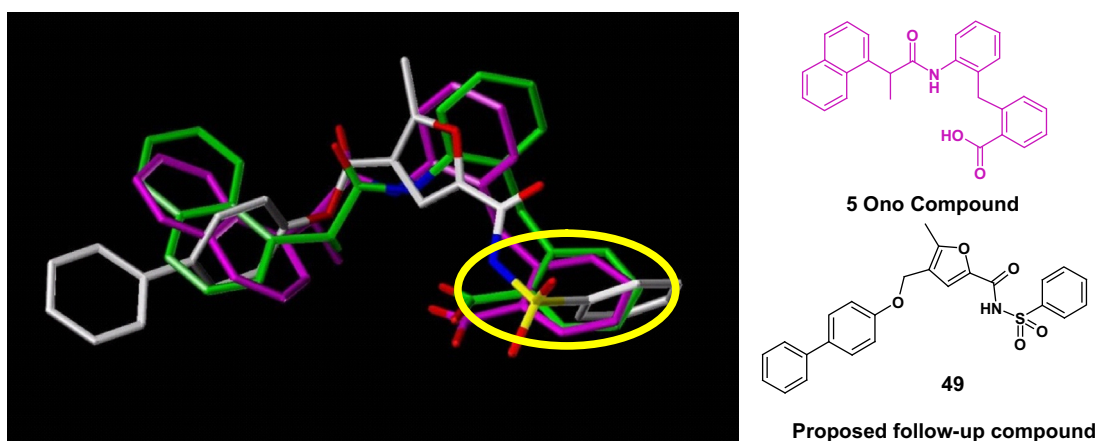


**Figure 5.** Superimposed FlexS overlay of (R/S)-Ono compound **5** with acyl sulfonamide derivative of lead carboxylic acid, **49**.

**Table 8**

Comparative selectivity data for Ono compound **5** with furan ether hit **6** and acyl sulfonamide derivative **49**

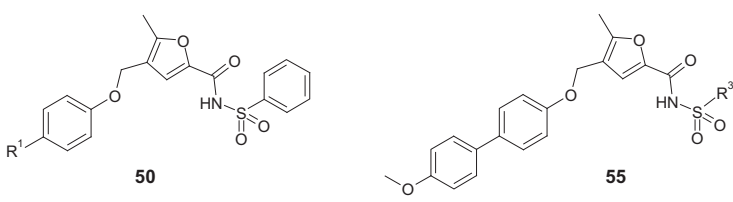
| Compound       | EP <sub>4</sub> R<br>K <sub>i</sub> (nM) | Fold-selectivity  |                   | LE/LLE    |
|----------------|--|-------------------|-------------------|-----------|
|                |  | EP <sub>2</sub> R | EP <sub>3</sub> R |           |
| <b>5</b> (Ono) | 7  | 630               | NT                | 0.36/2.46 |
| <b>6</b>       | 420                                      | 13                | 1000              | 0.35/1.66 |
| <b>49</b>      | 25                                       | 400               | 1000              | 0.31/2.57 |

NT = Not tested.

some 300-fold improvement over the original carboxylic lead **6**). A further series of analogues was prepared with variation to the acyl-sulfonamide substituent in compounds bearing the more potent *para*-methoxy biphenyl motif (compound **55**). The SAR of selected examples **56–61** indicated that, with the exception of the methyl analogue **56**, a wide degree of substitution was tolerated without being detrimental to EP<sub>4</sub>R affinity, and all potent compounds showed excellent EP<sub>4</sub>R/EP<sub>2</sub>R selectivity profiles.

The data in Table 9 highlight the improvement in EP<sub>4</sub>R affinity possible when moving from a carboxylic acid group in compound **6** to the acylsulfonamide in compounds typified by example **50**, which can be rationalised in our EP<sub>4</sub>R homology model using the related analogue **51** (Fig. 6). As well as compound **51** exhibiting similar hydrogen bonds to the those in carboxylic acid **6**, between Arg255 and the acylsulfonamide carbonyl group and between the ether linker and Tyr184 (see Fig. 2), an additional  $\pi$ -cation interaction with Lys272 and S=O interaction of the acyl sulfonamide moiety with Arg255 can also be seen. Moreover, the *para*-methoxy moiety in the biaryl group in **51** is in close proximity to Ser249 and Ser192 and could potentially form a hydrogen bond with either of these residues if a bridging water molecule (not in model) were present. The exquisite EP<sub>4</sub>R potency and EP<sub>4</sub>R/EP<sub>2</sub>R selectivity of the acylsulfonamide compounds, compared to their parent carboxylic acids, can be understood by a comparison of residue differences in the binding region of these receptors (key EP<sub>2</sub>R residues are shown in parentheses in Fig. 6). Clearly, the extra binding interactions possible for acylsulfonamide compounds in the EP<sub>4</sub>R with

**Table 9**  
Selected acylsulfonamide compounds



| Compound                     | R <sup>1</sup> | EP <sub>4</sub> R<br>K <sub>i</sub> (nM) | EP <sub>2</sub> R<br>Selectivity | Compound  | R <sup>3</sup> | EP <sub>4</sub> R<br>K <sub>i</sub> (nM) | EP <sub>2</sub> R<br>Selectivity |
|------------------------------|----------------|--|----------------------------------|-----------|----------------|--|----------------------------------|
| <b>6</b> (CO <sub>2</sub> H) |                | 420                                      | 13                               | <b>56</b> | Me             | 218                                      | NT                               |
| <b>49</b>                    |                | 25                                       | >1000                            | <b>57</b> | nPr            | 5.4                                      | >500                             |
| <b>51</b>                    |                | 5  | 1000                             | <b>58</b> |                | 11                                       | 650                              |
| <b>52</b>                    |                | 1.3                                      | 3890                             | <b>59</b> |                | 1.3                                      | >3000                            |
| <b>53</b>                    |                | 22                                       | >1000                            | <b>60</b> |                | 3.6                                      | 1500                             |
| <b>54</b>                    |                | 20                                       | >1000                            | <b>61</b> |                | 3  | >1000                            |

NT = not tested.

both Lys272, Arg255 (a bidentate interaction is now possible) and Ser192/249, which are not possible in EP<sub>2</sub>R, account for these marked differences.

The solubility data for selected acylsulfonamide compounds are shown in Table 10. These data for compounds with variation in the distal aromatic ring **50** show that, although very potent EP<sub>4</sub>R antagonists can be prepared (see Table 10, compounds **51** and **52**), the high lipophilicity has resulted in very poor aqueous solubility. Some improvements in solubility can be seen for the methoxy pyridine-containing analogue **53**—although a compromise on potency has been made. In our experience, further disruption of the planarity of biaryl rings by incorporation of a suitable *ortho* substituent has led to significant improvements in solubility. However, in this case, these were not realized (see compounds **62** and **63**). The solubility data for selected acylsulfonamide compounds having variation in the acylsulfonamide substituent **55** again indicated that highly potent examples were possible (dimethylisoxazole **59** K<sub>i</sub> = 1.3 nM; aqueous solubility = 0.2 μg/mL) but usually at the expense of aqueous solubility. The incorporation of polar elements failed to improve matters and, in many cases, led to a reduction in EP<sub>4</sub>R affinity. In order to identify candidate-quality molecules, an acceptable compromise had to be found.

In an attempt to boost the aqueous solubility of our potent acylsulfonamide compounds, selected amino-linked analogues were prepared (Table 11, entries **68**, **69** and **72**). Compound **68** exhibited encouraging solubility for an unsubstituted biphenyl analogue and a sevenfold increase in potency was achieved by optimising the acyl sulfonamide substituent to give example **69**. Ultimately, compound **72** was prepared which was found to have sub-nanomolar EP<sub>4</sub>R affinity (0.3 nM) and modest solubility (20 μg/mg). However, due to concerns over the perceived risk of releasing a biphenylamine moiety either chemically or metabolically in vivo, the amino-linked compounds were not profiled further. Finally, a compromise was found with compound **73**, which retained the ether linker, removing any biphenylamine risk, and incorporated

the *ortho*-tolyl acylsulfonamide substituent to improve primary EP<sub>4</sub>R affinity; the solubility of compound **73** was deemed acceptable for compound progression.

The aqueous solubility of compound **73** was further enhanced by formation of the sodium salt of the acylsulfonamide, which led to a marked improvement in solubility (>10 mg/mL). The sodium salt of compound **73** was designated **PGN1531**.

Profiling of **PGN1531** was undertaken to confirm that it was a functional antagonist at the EP<sub>4</sub>R. To this end, HEK-293 cells were prepared which stably expressed the human EP<sub>4</sub>R. **PGN1531** showed a concentration-dependent competitive antagonism of cAMP accumulation mediated by the action of the natural ligand, PGE<sub>2</sub>, on the EP<sub>4</sub>R with a pK<sub>b</sub> of 7.6.<sup>12</sup> Further investigation of **PGN-1531** was undertaken with native EP<sub>4</sub>Rs in human cerebral and meningeal arteries. **PGN-1531** was found to be a competitive antagonist of the PGE<sub>2</sub>-induced vasodilatation of human middle cerebral (pK<sub>B</sub> 7.8) and meningeal (pK<sub>B</sub> 7.6) arteries in vitro, but had no effect on responses induced by PGE<sub>2</sub> on coronary, pulmon-

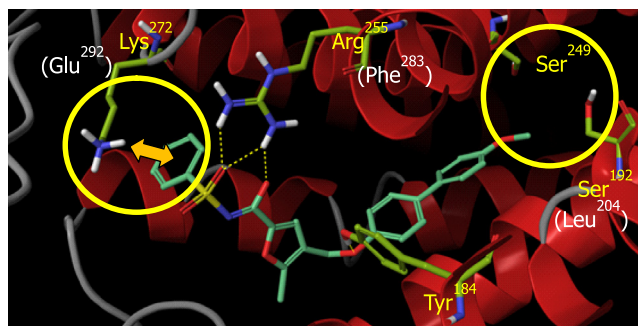
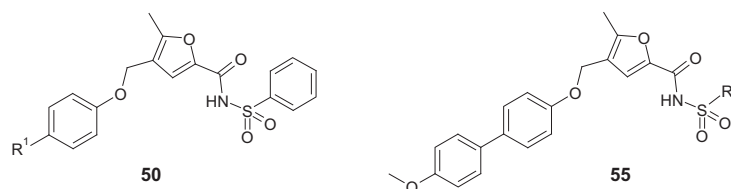


**Figure 6.** Binding mode of compound **51** (green) showing binding to key residues in the EP<sub>4</sub>R homology model—corresponding residues in the EP<sub>2</sub>R homology model are shown in white in parentheses.

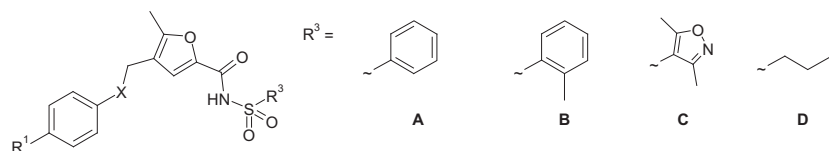
**Table 10**  
Solubility data for selected acylsulfonamide compounds



| Compound | R <sup>1</sup> | EP <sub>4</sub> R<br>K <sub>i</sub> (nM) | Solubility <sup>a</sup> 24 h (μg/mL) | Compound | R <sup>3</sup>           | EP <sub>4</sub> R<br>K <sub>i</sub> (nM) | Solubility <sup>a</sup> 24 h (μg/mL) |
|----------|----------------|--|--------------------------------------|----------|--------------------------|--|--------------------------------------|
| 49       |                | 25                                       | 2                                    | 58       |                          | 11                                       | 20                                   |
| 51       |                | 5  | 11                                   | 59       |                          | 1.3                                      | 0.2                                  |
| 52       |                | 1.3                                      | <0.6                                 | 64       |                          | 100                                      | <0.6                                 |
| 53       |                | 22                                       | 30                                   | 65       | <i>Me</i> <sub>2</sub> N | 115                                      | 10                                   |
| 62       |                | 21                                       | 20                                   | 66       |                          | 15                                       | 5                                    |
| 63       |                | 85                                       | 8                                    | 67       |                          | 1200                                     | 20                                   |

<sup>a</sup> Determinations carried out at RT in 0.1 M Phosphate Buffer/0.15 M KCl adjusted to pH 7.4. Sample determinations carried out in triplicate.

**Table 11**  
Optimising solubility and potency



| Compound | R <sup>1</sup> | Linker (X) | R <sup>3</sup> | EP <sub>4</sub> R<br>K <sub>i</sub> (nM) | Solubility <sup>a</sup> 24 h (μg/mL) |
|----------|----------------|------------|----------------|--|--------------------------------------|
| 68       |                | –NH–       | A              | 14                                       | 300                                  |
| 69       |                | –NH–       | B              | 2  | 20                                   |
| 70       |                | –O–        | D              | 5  | 7                                    |
| 71       |                | –O–        | C              | 0.6                                      | <0.6                                 |
| 72       |                | –NH–       | B              | 0.3                                      | 20                                   |
| 73       |                | –O–        | B              | 3  | 10                                   |
| 74       |                | –O–        | C              | 13                                       | 90                                   |
| 75       |                | –O–        | C              | 24                                       | 200                                  |

<sup>a</sup> Determinations carried out at RT in 0.1 M Phosphate Buffer/0.15 M KCl adjusted to pH 7.4. Sample determinations carried out in triplicate.

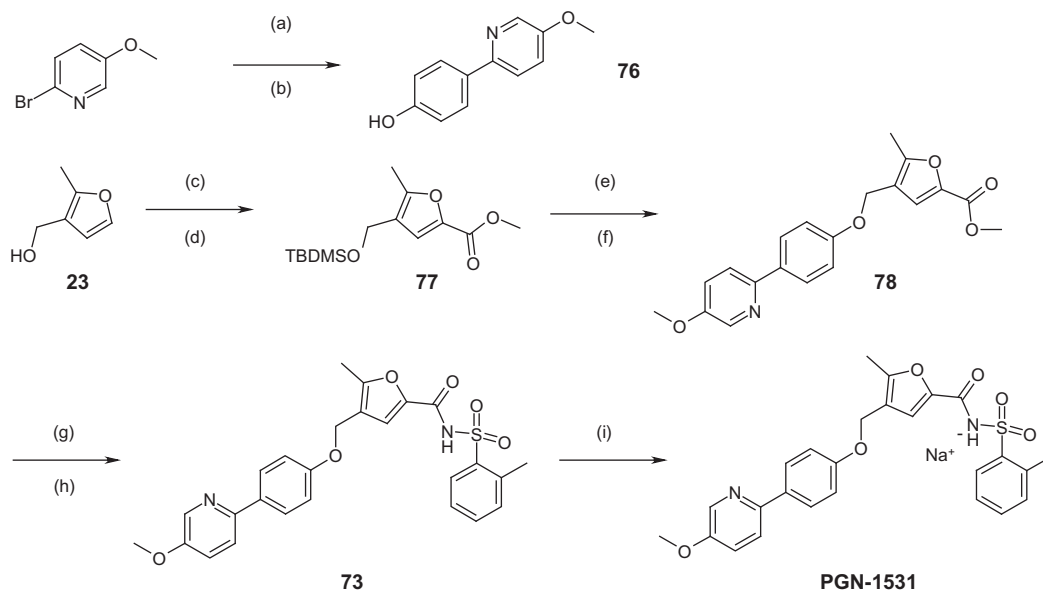
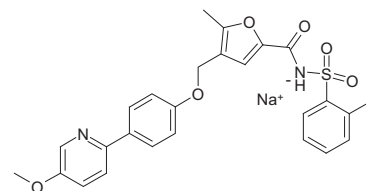
ary or renal arteries in vitro. In further tests, the compound showed no appreciable affinity at a wide range of other receptors (including other prostanoid receptors DP, FP, IP or TP), ion channels, transporters and enzymes ( $pK_i < 5$ ). **PGN-1531** (1–10 mg kg<sup>-1</sup> i.v.) was also shown to cause a concentration-dependent antagonism of the PGE<sub>2</sub>-induced increase in canine carotid blood flow in vivo,

thus demonstrating that an EP<sub>4</sub>R antagonist is able to reverse the vasodilatory effect of PGE<sub>2</sub> in an in vivo setting.<sup>12</sup>

The compound profile for **PGN-1531** is given in Table 12. The selection of this compound for clinical development was made following positive efficacy readouts in functional assays, very high EP<sub>4</sub>R/EP<sub>2</sub>R selectivity (high safety margin), excellent bioavailability

**Table 12**  
Compound profile for **PGN-1531**

| Property   | PGN-1531                |
|--|-------------------------|
| EP <sub>4</sub> R K <sub>i</sub> (nM)                      | 3                       |
| EP <sub>4</sub> R pK <sub>B</sub> (M) cAMP                 | 7.6                     |
| EP <sub>4</sub> R pK <sub>B</sub> (M) hum. Cerebral artery | 7.8                     |
| EP <sub>2</sub> R/EP <sub>3</sub> R selectivity            | >2500-fold              |
| c Log P/c log D/PSA (LE/LLE)                               | 4.1/2.2/114 (0.32/4.12) |
| Solubility (g/mL)  | >10                     |
| Caco-2 (nm/sec)  | 145                     |
| Human/Rat Int. Clearance (ml/min/kg)                       | 6.5 ± 1.4/2.7 ± 1.1     |
| Oral half-life(h)  | 2.3                     |
| Rat Bioavailability (%)                                    | 84                      |
| CYP inhibition (3A4, 2D6, 2C9, 1A2 and 2C19)               | None                    |
| CYP induction (CYP 3A4, 1A2)                               | None                    |
| PPB% (equilibrium dialysis)                                | 99.9                    |



**Scheme 2.** Synthesis of **PGN-1531**: (a) 4-(Benzyloxy)phenylboronic acid, PdCl<sub>2</sub>dppf, K<sub>2</sub>CO<sub>3</sub>(aq), Toluene, 80 °C, 18 h, (84%); (b) H<sub>2</sub>, 10% Pd/C, EtOH, RT, 1 h, (95%); (c) TBDMS-Cl, Imidazole, THF, RT, 5 h (93%); (d) (1) nBu-Li (1.3 M in hexanes), THF, –50 °C, 1 h, (2) Methyl chloroformate (80%); (e) TBAF, RT, 18 h (93%); (f) (1) Ms-Cl, Et<sub>3</sub>N, DCM, (2) **77**, Cs<sub>2</sub>CO<sub>3</sub>, DMF, RT, 18 h (80%); (g) NaOH(aq), EtOH, RT, 16 h (82%); (h) Toluene-2-sulfonamide, EDCI, DMAP, DCM, RT, 18 h (77%); (i) NaHCO<sub>3</sub>(aq), MeOH (95%).

in the rat, low intrinsic clearance in human hepatocytes and no CYP inhibition/induction issues.

Prior to progressing **PGN-1531** into clinical development, a robust synthetic route had to be found. The formal synthesis of **PGN1531** is given in [Scheme 2](#) and commenced with the preparation of compound **76**. Compound **76** was obtained using traditional Suzuki–Miyaura cross-coupling chemistry of 4-(benzyloxy)phenylboronic acid with 2-bromo-5-methoxy-pyridine, followed by removal of the benzyl protecting group by hydrogenation. The core furan template **23** was commercially available and after TBDMS-protection of the alcohol, lithiation with Bu–Li and quenching with methyl chloroformate, afforded the furan ester **77**. The silyl protecting group was removed using TBAF and the resulting alcohol converted to the mesylate under standard conditions. Coupling of the mesylate with the compound **76**, using basic conditions, gave the intermediate methoxy-pyridyl furan ester **78**. The hydrolysis of the ester and coupling of the resultant acid with *ortho*-toluenesulfonamide using EDCI afforded the acyl sulfonamide compound

**73**. The final stage of the synthesis involved the preparation of the sodium salt to improve the aqueous solubility—this was achieved with sodium bicarbonate in MeOH and gave **PGN-1531**. The route consists of 11 stages and gave an overall yield of 27%.

Following a successful multiple ascending oral dose phase 1a study with **PGN-1531**, additional clinical profiling was undertaken. In a phase 1b placebo-controlled study, the effects of two doses of the compound (200/400 mg p.o.) on UV<sub>B</sub> and capsaicin-induced neurogenic inflammation and hyperalgesia were assessed. To this end, the pain response to carbon dioxide laser pulses, applied directly to the irritated skin, was measured using EEG changes in somatosensory-evoked potentials (LSEP).<sup>17</sup> Gratifyingly, the peak-to-peak amplitudes in both pain paradigms were significantly reduced versus placebo, demonstrating a good overall analgesic response in both neurogenic and inflammatory pain models. These findings support further development of **PGN-1531** for the treatment of migraine.

In this Letter, we have presented the results of a hit-finding and lead optimisation programme against the EP<sub>4</sub>R. In a short time period, we were able to discover five structurally diverse series of hit compounds using a combination of virtual screening methods. The most favoured hit, compound **6**, was demonstrated to be a competitive antagonist of the EP<sub>4</sub>R. Compound **73** was identified following several rounds of optimization, which centered on improving both the primary EP<sub>4</sub>R affinity and selectivity against the related EP<sub>2</sub>R as well as the aqueous solubility.<sup>18</sup> This work culminated in the preparation of **PGN-1531**, the sodium salt of **73**, which showed marked improvements in solubility (>10 mg/mL). **PGN-1531** is a potent and selective antagonist at EP<sub>4</sub>Rs in vitro and in vivo, with the potential to alleviate the symptoms of migraine that result from cerebral vasodilatation.

### Acknowledgments

The authors wish to thank Mike Podmore and Russell Scammell for analytical support and George Hynd for assistance in the generation of early library samples.

### References and notes

- (a) Hata, A. N.; Breyer, R. M. *Pharmacol. Ther.* **2004**, *103*, 147; (b) Daniel Flesch<sup>†</sup>; Daniel Merk; Christina Lamers; Manfred Schubert-Zsilavecz *Expert Opin. Ther. Pat.* **2013**, *23*, 233.
- (a) Coleman, R. A. et al The IUPHAR Compendium of Receptor Characterization and Classification, 2nd ed.; IUPHAR Media: London, UK, 2000. pp 337–353; (b) Sugimoto, Y.; Narumiya, S. *J. Biol. Chem.* **2007**, *282*, 11613.
- Lin, C.-R.; Amaya, F.; Barrett, L.; Wang, H.; Takada, J.; Samad, T. A.; Woolf, C. J. *J. Pharmacol. Exp. Ther.* **2006**, *319*, 1096.
- Davis, R. J.; Murdoch, C. E.; Ali, M.; Purbrick, S.; Ravid, R.; Baxter, G. S.; Tilford, N.; Sheldrick, R. L. G.; Clark, K. L.; Coleman, R. A. *Br. J. Pharmacol.* **2004**, *141*, 580.
- Abramovitz, M.; Adam, M.; Boie, Y.; Carriere, M.-C.; Denis, D.; Godbout, C.; Lamontagne, S.; Rochette, C.; Sawyer, N.; Tremblay, N. M.; Belley, M.; Gallant, M.; Dufresne, C.; Gareau, Y.; Ruel, R.; Juteau, H.; Labelle, M.; Ouimet, N.; Metters, K. M. *Biochim. Biophys. Acta* **2000**, *1483*, 285.
- Clayton, N. M.; Collins, S. D.; Foord, S. M.; Giblin, G. M. P. PCT Int. Appl. WO2001/010426 A2, 2001.
- Juteau, H.; Gareau, Y.; Labelle, M.; Lamontagne, S.; Tremblay, N.; Carriere, M.-C.; Sawyer, N.; Denis, D.; Metters, K. M. *Bioorg. Med. Chem. Lett.* **2001**, *11*, 747.
- Hattori, K.; Tanaka, A.; Kono, Y.; Nakazato, S. PCT Int. Appl. WO2000/018744 A1, 2000.
- Machwate, M.; Harada, S.; Leu, C. T.; Seedor, G.; Labelle, M.; Gallant, M.; Hutchins, S.; Lachance, N.; Sawyer, N.; Slipetz, D.; Metters, K. M.; Rodan, S. B.; Young, R.; Rodan, G. A. *Mol. Pharmacol.* **2001**, *60*, 36.
- Tani, K.; Kobayashi, K.; Maruyama, T. PCT Int. Appl. WO2001/062708 A1, 2001.
- Primary assays*: Membranes were prepared from cells stably transfected with human EP<sub>4</sub> receptor cDNA. In brief, cells were cultured to confluency, scraped from culture flasks, and centrifuged (800 g, 8 min, 4 °C). Cells were twice washed in ice cold homogenisation buffer containing 10 mM Tris-HCl, 1 mM EDTA-Zn, 250 mM sucrose, 1 mM PMSF, 0.3 mM indomethacin, pH 7.4, homogenised and re-centrifuged as before. The supernatant was stored on ice and pellets re-homogenised and re-spun. Supernatants were pooled and centrifuged at 40,000g, 10 min, 4 °C. Resultant membrane pellets were stored at -80 °C until use. For assay, membranes expressing human EP<sub>4</sub>, EP<sub>3</sub>, EP<sub>2</sub> or EP<sub>1</sub> receptors were incubated in Millipore (MHVBN45) plates containing assay buffer, radiolabelled [<sup>3</sup>H] PGE<sub>2</sub> and 0.1–10,000 nM concentrations of compounds. Incubations were performed at suitable temperatures and for suitable times to allow equilibrium to be reached. Non-specific binding was determined in the presence of 10 μM PGE<sub>2</sub>. Bound and free radiolabel was separated by vacuum manifold filtration using appropriate wash buffers, and bound radiolabel was determined by scintillation counting. The affinity or pK<sub>i</sub> of each compound for each receptor was calculated from the concentration causing 50% radioligand displacement (IC<sub>50</sub>) by using the Cheng-Prusoff equation.
- Maubach, K. A.; Davis, R. J.; Clark, D. E.; Fenton, G.; Lockey, P. M.; Clark, K. L.; Oxford, A. W.; Hagan, R. M.; Routledge, C.; Coleman, R. A. *Br. J. Pharmacol.* **2009**, *156*, 316.
- (a) *Homology modeling carried out using Prime, version 3.1*; Schrödinger, LLC: New York, NY, 2012; (b) Jacobson, M. P.; Pincus, D. L.; Rapp, C. S.; Day, T. J. F.; Honig, B.; Shaw, D. E.; Friesner, R. A. *Proteins: Struct. Funct. Bioinf.* **2004**, *55*, 351; (c) Jacobson, M. P.; Friesner, R. A.; Xiang, Z.; Honig, B. *J. Mol. Biol.* **2002**, *320*, 597.
- (a) *Ligand docking carried out using Glide, version 5.8*; Schrödinger, LLC: New York, NY, 2012; (b) Friesner, R. A.; Murphy, R. B.; Repasky, M. P.; Frye, L. L.; Greenwood, J. R.; Halgren, T. A.; Sanschagrin, P. C.; Mainz, D. T. *J. Med. Chem.* **2006**, *49*, 6177; (c) Halgren, T. A.; Murphy, R. B.; Friesner, R. A.; Beard, H. S.; Frye, L. L.; Pollard, W. T.; Banks, J. L. *J. Med. Chem.* **2004**, *47*, 1750; (d) Friesner, R. A.; Banks, J. L.; Murphy, R. B.; Halgren, T. A.; Klicic, J. J.; Mainz, D. T.; Repasky, M. P.; Knoll, E. H.; Shaw, D. E.; Shelley, M.; Perry, J. K.; Francis, P.; Shenkin, P. S. *J. Med. Chem.* **2004**, *47*, 1739.
- (a) *SiteMap, version 2.7*; Schrödinger, LLC: New York, NY, 2013; (b) Halgren, T. J. *J. Chem. Inf. Model.* **2009**, *49*, 377; (c) Halgren, T. *Chem. Biol. Drug Des.* **2007**, *69*, 146.
- (a) FlexS, BioSolveIT GmbH, An der Ziegelei 79, 53757 Sankt Augustin, Germany.; (b) Lemmen, C.; Lengauer, T.; Klebe, G. *J. Med. Chem.* **1998**, *41*, 4502.
- Master, F. R.; Peachey, M. C.; Graham, C.; Routledge, C. Analgesic effect of the novel, potent and selective prostanoid EP<sub>4</sub>R antagonist, BGC20-1531: a placebo-controlled study using laser-induced somatosensory-evoked potentials obtained from UV<sub>B</sub> and capsaicin irritated skin in healthy volunteers. Poster presented at 18th International Headache Research Seminar, 6–8th March 2009, Copenhagen, Denmark.
- Clark, D.; Clark, K.; Coleman, R.; Davis, R.; Fenton, G.; Harris, N.; Hynd, G.; Newton, C.; Oxford, A.; Stuttle, K.; Sutton, J. PCT Int. Appl. WO2004/067524 A1, 2004.